Geological Society of America
Special Paper 196
1984

REE and Nd isotopes in conodont apatite: Variations with geological age and depositional environment

Judith Wright
Department of Geology
University of Oregon
Eugene, Oregon 97403

Richard S. Seymour
EG and G Ortec
100 Midland Road
Oak Ridge, Tennessee 37830

Henry F. Shaw
The Lunatic Asylum of the
Charles Arms Laboratory
Division of Geological and Planetary Sciences
California Institute of Technology
Pasadena, California 91125

ABSTRACT

Modifications of standard instrumental neutron activation analysis procedures have produced quantitative results for REE, Th, and U contents of the biogenically precipitated apatite of conodonts and ichthyoliths. These results are in agreement with isotopic studies of four of the samples. Apatite of modern fish debris apparently concentrates REE during early diagenesis in the same proportions as seawater, and therefore carries a signature of the oceanic REE pattern, suggesting the same relationship between fossil apatite and ancient seas. REE patterns of conodont samples from Cambrian through Triassic times show significant secular variations. Further, these data show that REE vary among depositional settings; e.g., fauna from continental shelf biofacies vs. epicratonic seas, and are consistent among fauna from the same depositional framework.

In the modern oceanic environment, cerium is preferentially scavenged by hydrous iron oxides resulting in a negative Ce anomaly in seawater REE patterns. This Ce-Fe affinity leads to an analysis of changing oxidation-reduction conditions in ancient seas that explains the variations in Ce_{anom} of conodonts. During times of widespread anoxia in the water column, dissolution of Fe oxides would release Ce to produce an enrichment of Ce in the water column, effectively removing the negative Ce anomaly, and at times even causing a positive Ce anomaly. These anoxic events are recorded by a small or absent Ce_{anom} of conodonts during the Lower Paleozoic and again in the Triassic. Variations in Ce_{anom} appear to be related to Th/U variations, another potential indicator of redox changes. Fossil apatite of conodonts records Nd and Sr isotopic variations in ancient seawater.

INTRODUCTION

Clues to the chemical and physical evolution of ancient oceans are found in sedimentary clastic and chemically precipitated rocks of Archean to Proterozoic times. These seas provided a set of circumstances that permitted the origin of life. As primordial organisms evolved, their interaction with the environment produced changes not only in the hydrosphere, but also in the atmosphere, and possibly set the stage for more complex life forms to develop (Berry and Wilde, 1983). Although many geochemists assume a constant oceanic composition from late in the Proterozoic to the present, isotopic composition versus age curves of carbon and sulfur imply changes in the distribution of oxidized and reduced species in the exogenic cycles of these elements throughout the Phanerozoic (Veizer et al., 1980). Near the Proterozoic-Phanerozoic boundary, marine organisms evolved that precipitated inorganic mineral constituents as endo- and exoskeletons. This development was undoubtedly significant for the cycles of some ionic species in seawater. Incorporation of major and trace ions into the carbonaceous, siliceous, and phosphatic hard parts of the biota effectively removed them from other interactions in the oceanic reservoir (Lowenstam, 1974; Lowenstam and Weiner, 1983). These considerations have led us to search for chemical and isotopic clues retained in the phosphatic fossil remains of conodonts, organisms that inhabited Cambrian through Triassic seas. Perhaps the trace element (TE) chemistry of conodonts will help us to a better understanding of changes in the ocean during Paleozoic times.

ANALYTICAL PROCEDURES

Instrumental Neutron Activation Analysis

Instrumental neutron activation analysis (INAA) is a non-destructive and highly sensitive technique which permits elemental abundances to be determined rapidly and accurately. INAA is a quantitative application of gamma-ray spectroscopy measuring *decay* gammas associated with beta decay of unstable daughter nuclides produced by a neutron capture reaction (n, γ). This technique was chosen for chemical studies of conodonts because 1) relatively small mass samples can be analyzed; 2) 20-30 elements may be determined at μg/g concentrations; 3) the technique is non-destructive so that the sample may be re-used for a variety of other analytical methods (although isotopic ratios are perturbed); and 4) a large number of samples may be analyzed in a single experiment. Comparative INAA was first described by Gordon et al. (1968) with additional discussions of the technique by Muecke (1980), and Brunfeldt and Steinnes (1971). INAA was first applied to conodonts by Bradshaw et al. (1973).

We use a modification of the approach described by Gordon. Two different sets of experimental conditions at the University of Oregon, Eugene, and NASA-JSC, Houston, were used in this work. Results from samples that were run under both sets of experimental conditions are comparable.

The following modifications are particularly important in biomineral analysis:

1) Type of conodont samples. We decided to use composite samples of all types of conodonts from a specific biostratigraphic horizon (Table 1). The underlying assumption is that the use of composite samples minimizes metabolic effects on the genus, species, or individual level, and gives a more accurate *average* sampling of the seawater and depositional environment (such as seawater composition) in which the group of organisms lived.

2) Clean preparation techniques. All conodont samples are cleaned ultra-sonically in absolute ethanol to remove adhering detritus.

3) Weighing of samples. We use an electronic semi-micro balance with an accuracy of ± 0.01 mg, and average a set of three weighings. Each sample contains from 12 to 600 pieces of fossil material and ranges in weight from 0.21 to 12.0 mg.

4) Sample containers. High-purity silica glass tubes (Supersil) with extremely low and well-known TE concentrations are used as sample containers.

5) Irradiation of samples. Experiments 57, 59, and 63 at the University of Oregon (Table 1) were irradiated in General Dynamics TRIGA Reactor at Oregon State University Nuclear Center for a total fluence of 2×10^{17}n cm^{-2}. Experiments 184, 192, 193, and 204 at NASA-JSC in Houston, were irradiated in General Dynamics TRIGA Reactor at Texas A&M University Nuclear Center for a total fluence of 1×10^{18}n cm^{-2}. The increased neutron dosage at NASA has allowed us to decrease sample size by an order of magnitude from 1-9 mg of sample to <1 mg.

Isotopic Analysis

Milligram-size (see Table 2) conodont samples and one sample of modern shark's teeth were dissolved in dilute HCl. The solutions were spiked for isotope dilution analysis with ^{87}Rb, ^{84}Sr, ^{147}Sm and ^{150}Nd using the INAA concentration data as a guide, so that both isotopic composition and concentration could be determined precisely on the same aliquot. After centrifuging to remove insoluble organic material, Rb, Sr, Sm and Nd were separated from the sample solution using standard ion-chromatographic techniques. Details of the chemical procedure and mass spectrometric techniques are given in Papanastassiou et al. (1977), DePaolo (1978), and Shaw (1984). Chemical blanks for this procedure are ~40 pg Nd and ~200 pg Sr, and are negligible. The errors quoted in Table 2 for the isotopic ratios correspond to 2σ of the mean of ~200 ratios for Nd and ~150 ratios for Sr. The uncertainties given in Table 2 for the Sm/Nd and Rb/Sr ratios result only from uncertainties in spike calibrations and in run statistics.

Sample Distribution

Geographic distribution of samples is shown in Figure 1 and the system, stage, location, and formation of each sample is listed in Table 1. The large number of samples from the continental

TABLE 1. AGE AND LOCATION OF CONODONT AND ICHTHYOLITH SAMPLES

Sample	System	Stage	Location	Fm.	Donor	Type
JWC20-6	Recent		Coos Bay, OR	N.W. Pacific coastal waters	caught by J.W.C.	shark teeth
JW6	L. Triassic	Smithian-Spathian	Weber Cyn, Utah	Thaynes Fm.	D.L. Clark	conodonts, fish
JWC56	"	"	Salt Lake City, Utah	"	"	"
JWC9-1	"	middle Smithian	Nev.	"	"	"
JW5	U. Permian	Upper Guadalupian	Culbertson Co. Texas	Pinery Fm.	"	"
JWC54	"	"	"	"	"	fish
JWC51	U. Pennsyulvanian	Virgilian	Muskingum Co. Ohio	Ames Ls.	J. Kovach	conodonts
JWC50	"	"	"	"	"	"
JWC47	"	"	Allegheny Co. Pennsylvania	"	"	"
JWC46	"	"	Guernsey Co. Ohio	"	"	"
JWC45	Pennsylvanian	U. Missourian	"	Portersville Ls.	"	"
JWC41	M. Pennsylvanian	L. Desmoinesian	Henry Co. Illinois	Spoon Fm. Seville Mbr.	"	"
JWC52	"	"	White Pine Co. Nevada	basal Riepe Springs	D.L. Clark	"
JWC53	"	"	"	"	"	fish
JW4	"	"	"	"	"	conodonts, fish
JWC43	L. Pennsylvanian	M. Atokan	Greendale, Ohio	L. Mercer Ls.	M.T. Sturgeon	conodonts
JWC40	U. Mississippian	L. Chesterian	San Saba, Texas	Barnett Fm.	G.K. Merrill	"
JW3	L. Mississippian	Osagean	Lincoln Co. Wyoming	Mission Cyn. Fm.	D.L. Clark	conodonts
JWC6-1	Mississippian		Lancashire England	unknown	M.J. Reynolds	"
JWC39	L. Mississippian	U. Kinder-hookian	Indiana	New Albany Shale	C.B. Rexroad	"
JWC38	"	"	"	"	"	"
JWC37	"	M. Kinder-hookian	Crawford Mtns. Wyoming	Lodgepole Limestone	C.A. Sandberg	"
JWC36	"	"	St. Genevieve Co. Missouri	Bushberg Sandstone	"	"
JWC35	"	"	Bighorn Co. Wyoming	Madison Limestone	"	"
JWC5-1	U. Devonian	Famennian	Missouri	Holt Summit Sandstone	R.L. Ethington	conodonts
JWC34	"	"	Lincoln Co. Nevada	Pilot Shale	C.A. Sandberg	"
JWC33	"	"	"	"	"	"
JWC32	"	Frasnian	Nevada	Devil's Gate Limestone	"	"
JWC30	"	"	Erie Co. N.Y.	Genesee Fm. Genundewa Mbr.	C.T. Helfrich	"
JWC29	"	"	Speed Indiana	New Albany Shale	C.B. Rexroad	"

TABLE 1. AGE AND LOCATION OF CONODONT AND ICHTHYOLITH SAMPLES (continued)

Sample	System	Stage	Location	Fm.	Donor	Type
JWC28	M. Devonian	Givetian	Bartholomew Co. Indiana	"	C.A. Sandberg	"
JWC27	"	Eifelian	Delaware Co. Ohio	Delaware Limestone	W.C. Sweet	"
JWC26	"	"	"	"	"	"
JWC25	"	"	White Sulfur Ohio	Columbus Limestone	"	"
JWC24	L. Devonian	Gedinnian	Nevada	unknown	S.G. Barnett	"
JW9	"	"	Klamath Mtns. California	unnamed	N.M. Savage	"
JWC23	U. Silurian	U. Ludlovian	Sunnyhill Wuarry England	U. Bringewood Fm.	C.B. Rexroad	"
JWC4-1	L. Silurian	Wenlockian	England	unknown	R.J. Aldridge	"
JW8	"	"	Death Valley California	Hidden Valley Dolomite	R.H. Miller	"
JWC10	"	"	Cap Island, Alaska	unnamed	N.M. Savage	"
JWC11	"	"	Carnic Alps, Austria	"	"	"
JWC22	"	Llandoverian	Bath Co. Kentucky	Brassfield Fm.	C.T. Helfrich	"
JWC21	"	"	Adams Co. Ohio	"	W.C. Sweet	"
JWC20	U. Ordovician	L. Ashgillian	Clark Co. Kentucky	Ashlock Fm.	"	"
JWC19	"	"	"	"	"	"
JWC18	"	U. Caradocian	Richmond Kentucky	Calloway Creek Limestone	C.T. Helfrich	"
JWC17	"	L. Caradocian	Fittstown Oklahoma	Corbin Ranch Formation	W.C. Sweet	conodonts, fish
JW2	M. Ordovician	U. Llandeilian	Western Dane Co. Wisconsin	L. Galena Fm.	D.L. Clark	conodonts
JWC16	"	Llandeilian	Fittstown, Oklahoma	Tulip Crk. F.	"	"
JWC3-16	"	Llanvirnian	Öland, Sweden	unknown	Klaus Müller	"
JWC15	"	"	Carter Co. Oklahoma	Mclish Fm.	W.C. Sweet	"
JWC14	"	"	"	Joins Fm.	"	"
JWC3-34	L. Ordovician	Tremadocian	Chandler Crk. section, Okla.	Signal Mtn. Fm.	collected with J.F. Miller	"
JWC3-24	"	"	Lange Ranch Section, Texas	Wilbern Fm. San Saba Mbr.	"	"
JW7	U. Cambrian	Dresbachian	Ash Meadows, Nevada	Dunderberg Shale	R.H. Miller	"

TABLE 2. CONODONT Nd,Sr ISOTOPIC DATA

Sample	Wt (mg)	ppm Nd	Sm/Nd[1]	$f^{Sm/Nd}$	$^{143}Nd/^{143}Nd$[2]	$\varepsilon_{Nd}(T)$[3]	ppm Sr	Rb/Sr[4]	$f^{Rb/Sr}$	$^{87}Sr/^{86}Sr$[5]	$\varepsilon_{Sr}(T)$[3]
JWC-35	2.02 ±0.04	183.8	0.221	-0.321	0.51134 ±0.00002	-7.1 ±0.4	3640	2.63×10^{-4}	-0.991	0.70802 ±0.00005	+55.6 ± 0.8
JWC-37	2.02 ±0.04	166.2	0.211	-0.352	0.51138 ±0.00002	-6.0 ±0.4	2855	5.32×10^{-4}	-0.981	0.70807 ±0.00003	+56.3 ± 0.5
JWC-32	6.18 ±0.04	81.3	0.199	-0.390	0.51132 ±0.00002	-6.8 ±0.4	4080	9.07×10^{-5}	-0.997	0.70812 ±0.00004	+57.2 ± 0.6
JWC-30	3.37 ±0.04	171.4	0.348	+0.059	0.51152 ±0.00002	-6.9 ±0.4	2655	5.35×10^{-4}	-0.981	0.70784 ±0.00004	+53.2 ± 0.6
Ph-02[6]	1061.48 ±0.04	5×10^{-3}	0.145	-0.570	....	...	....	....	....	....	...

Note: f explained in text.
[1]Uncertainty = 0.4%.
[2]Normalized to $^{146}Nd/^{144}Nd = 0.636151$.
[3]Initial ε values calculated using the following ages: JWC-35 and JWC-37, T = 342±3 My; JWC-32, T = 352±3 My; JWC-30, T = 357±3 My. Errors on ε(T) include both analytical error and error due to age uncertainty.
[4]Uncertainty = 1.0%.
[5]Normalized to $^{86}Sr/^{88}Sr = 0.1194$.
[6]Shark's teeth from Bull Shark collected November 1965 in Mazatlan, San Juan, Mexico, by H. Lowenstam.

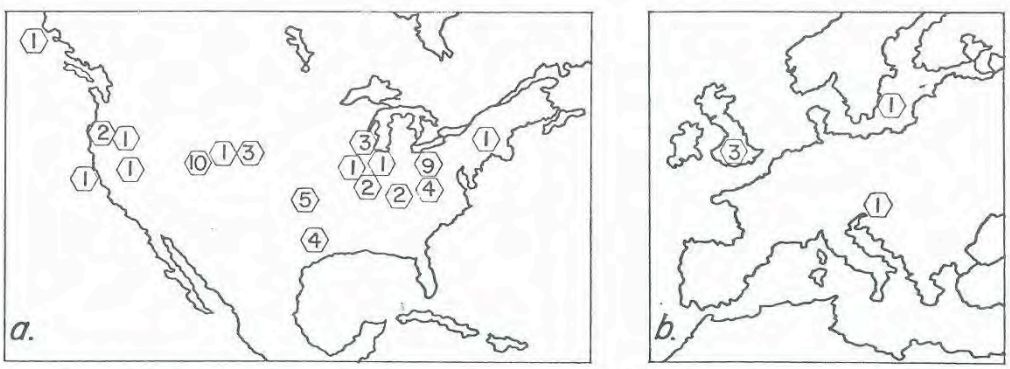

Figure 1. Distribution of sample locations; number within symbol indicates number of samples at each general location: (a) United States, (b) Western Europe.

United States allows a concrete comparison of the chemical variations of conodonts among provinces; e.g., Pacific and Proto-Atlantic continental margins, and epicratonic seas.

RESULTS AND DISCUSSION

Representation of INAA Data

Concentrations in ppm, and 1 σ errors, of Th, U and 8 of the rare earth (lanthanide) element (REE) group, La, Ce, Nd, Sm, Eu, Tb, Yb, and Lu are listed in Appendix 1. Conventionally, REE are not displayed as absolute abundances, but are normalized element by element to a standard chosen as compatible with the system under study. We use the North American Shale Composite (NASC) standard (Haskins et al., 1968). The normalization process removes the odd-even effect of elemental distributions and produces a smoothed curve in which it is relatively simple to recognize significant enrichments or depletions of one or more of the REE. Normalized concentrations are plotted on a logarithmic scale versus atomic number, to produce a REE pattern (also called a fingerprint or signature) for each sample. Visual comparison of REE patterns among samples permits immediate recognition of variations in the REE signature. In Figure 2, REE patterns are grouped by system for Cambrian through Triassic samples.

Representation of Isotopic Data

The naturally occurring radioactive isotopes ^{87}Rb and ^{147}Sm decay with half-lives $\tau_{1/2}^{Rb} = 49$ AE and $\tau_{1/2}^{Sm} = 106$ AE to

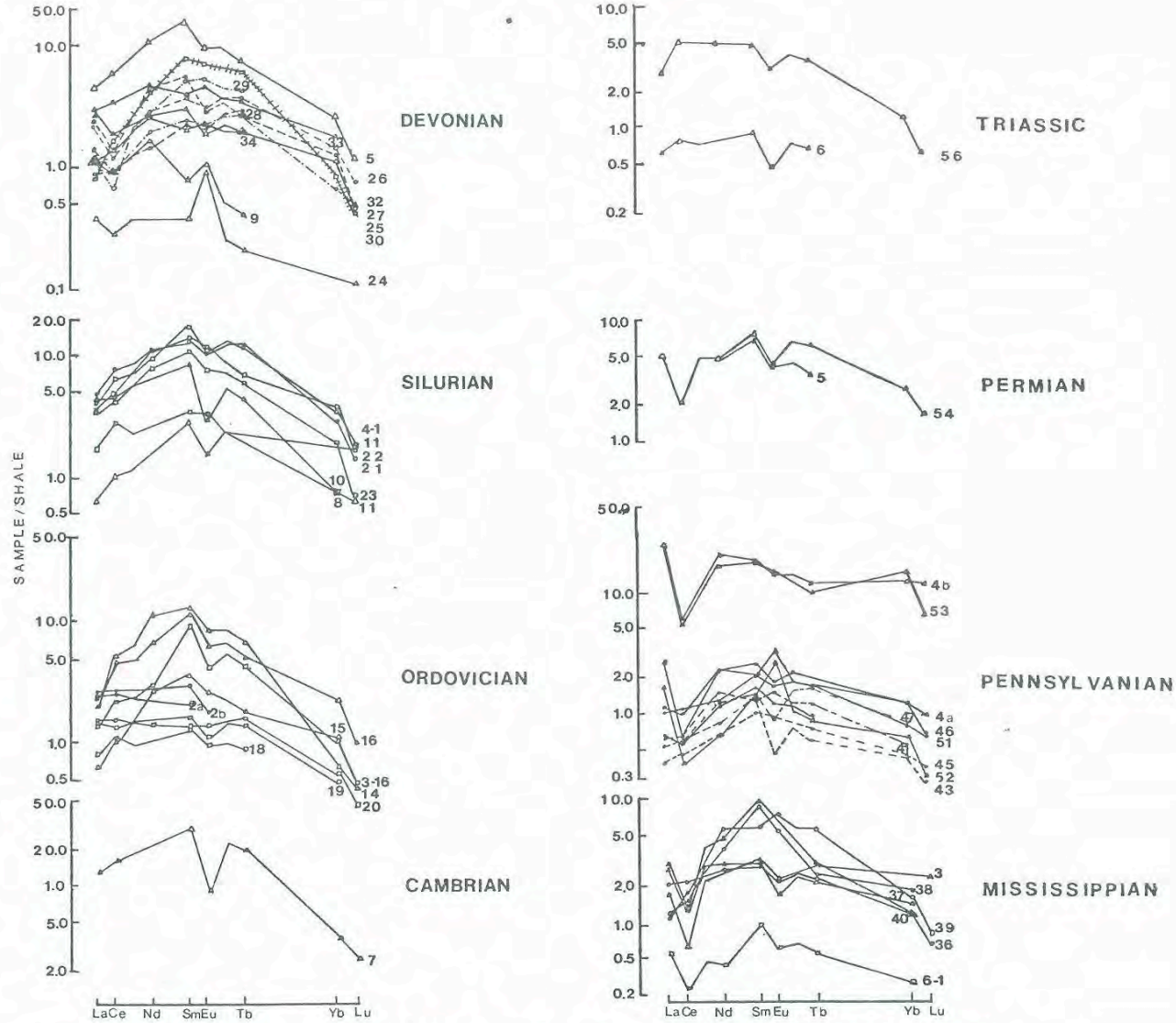

Figure 2. Shale-normalized REE in conodont samples of Cambrian through Triassic age. Sample numbers as listed in Table 1 without JWC prefix.

the respective daughter isotopes ^{87}Sr and ^{143}Nd. Closed systems with differing initial parent-to-daughter ratios will evolve over time and develop measurable differences in the daughter-element isotopic abundances. It is convenient to represent Nd isotopic data in terms of epsilon notation (DePaolo and Wasserburg, 1976) in which $\epsilon_{Nd}(T)$ is the deviation in parts in 10^4 of the sample isotopic composition from a nominal chondritic reservoir at time T.

$$\epsilon_{Nd}(T) = [\,(\frac{^{143}Nd}{^{144}Nd})_{\text{Sample}}(T)/(I_{CHUR}(T)) - 1] \times 10^4$$

where $I_{CHUR}(T) = I_{CHUR}(0) - (\frac{^{147}Sm}{^{144}Nd})_{CHUR} \cdot [\exp(\lambda^{Sm} \cdot T) - 1]$; $\lambda^{Sm} = 6.54 \times 10^{-12}$ yr^{-1}, $I_{CHUR}(0) = 0.511847$, $(^{147}Sm/^{144}Nd)_{CHUR} = 0.1967$ (DePaolo and Wasserburg, 1976; Jacobsen and Wasserburg, 1980; Wasserburg et al., 1981).

Similarly, one may define $\epsilon_{Sr}(T)$ with respect to a nominal undepleted mantle or bulk earth reservoir:

$$\epsilon_{Sr}(T) = [\,(\frac{^{87}Sr}{^{86}Sr})_{\text{Sample}}(T)/I_{UR}(T) - 1] \times 10^4$$

where $I_{UR}(T) = I_{UR}(0) - (^{87}Rb/^{86}Sr)_{UR} \cdot [\exp(\lambda^{Rb} \cdot T) - 1]$; $\lambda^{Rb} = 1.42 \times 10^{-11}$ yr^{-1}, $I_{UR}(0) = 0.7045$, $(^{87}Rb/^{86}Sr)_{UR} = 0.0827$ (DePaolo and Wasserburg, 1976; O'Nions et al., 1977). The Sm/Nd and Rb/Sr ratios may also be referenced to these

model reservoirs by defining the enrichment factors

$$f^{Sm/Nd} = [(\frac{^{147}Sm}{^{144}Nd})_{Sample} / (\frac{^{147}Sm}{^{144}Nd})_{CHUR} - 1]$$

and

$$f^{Rb/Sr} = [(\frac{^{87}Rb}{^{86}Sr})_{Sample} / (\frac{^{87}Rb}{^{86}Sr})_{UR} - 1].$$

Table 2 lists $\epsilon_{Nd}(T)$, $\epsilon_{Sr}(T)$, $f^{Sm/Nd}$ and $f^{Rb/Sr}$ calculated for the samples we have analyzed.

General Trends

In order to sort out the variations among the patterns, it is customary to examine each half of the REE pattern separately; i.e., the light lanthanides, lanthanum to gadolinium (atomic numbers 57 to 64) and the heavy lanthanides, gadolinium to lutetium (atomic numbers 64 to 71). Two significant variations apparent among the light lanthanide portion of the REE patterns involve cerium and europium (Figure 2). When either element is enriched, its position in the overall pattern is higher than neighboring elements; conversely, depletion is signified by a lower position in the pattern relative to neighboring elements.

Members of the REE group have a similar ionic radius and +3 valence states, with the exception of Ce and Eu whose valence states can vary under differing oxidation-reduction conditions: $Ce^{3+} \rightarrow Ce^{4+}$, $Eu^{2+} \rightarrow Eu^{3+}$. Therefore, it is generally assumed that anomalous variations in these elements are due to changes in the oxidation state of the system under consideration.

The conodont REE patterns show many perturbations in Ce and Eu (Figure 2). Cambrian through Silurian samples have no depletion of Ce, but in the majority of Devonian through Permian samples a significant Ce depletion is present—a negative Ce anomaly. In Triassic samples Ce is present once again in normal or non-depleted amounts. Eu does not follow consistent trends; sometimes it is depleted when Ce is depleted, and sometimes when Ce is not. Eu variations must be more complex and involve factors whose nature we do not understand at present. The group of samples reported here represents a survey of variations throughout conodont time. Detailed and stratigraphically well-controlled studies of time slices are now in progress and may reveal a more accurate picture of the significance of Eu variations.

The heavy lanthanide portion of the patterns shows pronounced variations in slope. Some patterns have steep negative slopes reminiscent of the heavy lanthanide pattern for old crustal granitic rocks (Haskins and Paster, 1979), and some have shallow to nearly horizontal negative slopes reminiscent of the heavy lanthanide patterns for volcanic rocks. Slopes intermediate to these types may reflect a mixed source (Taylor and McLennon, 1981). This suggests that the heavy lanthanide contents of the conodont REE patterns may be strongly influenced by differing erosional provenances or inputs such as mid-ocean ridge basalts (MORB), to the seawater system that nurtured the conodont animal.

Nd and Sr isotopic analyses of conodonts may help to determine the source of the REE which were ultimately incorporated into the conodonts. Recent work on the Nd isotopic composition of modern seawater has shown that because of the short residence time of Nd in seawater (~100-1000 years) there are distinct differences in the $^{143}Nd/^{144}Nd$ isotopic ratio between different major ocean basins, but that internally each basin is relatively homogeneous. The range of ϵ_{Nd} (0) values for water in different ocean basins is shown in Table 3 (Piepgras et al., 1979; Piepgras and Wasserburg, 1980, 1982; Goldstein and O'Nions, 1981). The estimated averages of ϵ_{Nd} (0) for these oceans are: Atlantic Ocean, –12; Indian Ocean, –8; Pacific Ocean, –3. For comparison, Table 3 lists typical ranges of ϵ_{Nd} (0) for possible crustal and mantle sources for the Nd in seawater. It is clear from this comparison that Nd in seawater is derived mainly from old continental crust (ϵ_{Nd} (0) <0), and that there is little contribution from sources with a depleted oceanic mantle isotopic signature (ϵ_{Nd} (0) ~ +10) such as mid-ocean ridge basalts. The fact that Atlantic seawater has more negative ϵ_{Nd} (0) values relative to Pacific seawater must reflect the greater importance of old continental crustal sources relative to young volcanic sources for Nd injection into the Atlantic Ocean. By analyzing the Nd isotopic composition of conodonts, it may thus be possible to constrain the ultimate source of the REE in conodonts and more importantly, to determine variations in ϵ_{Nd} (T) in ancient ocean water, in a manner similar to published seawater Sr isotopic curves (Peterman et al., 1970; Dasch and Biscaye, 1971; Veizer and Compston, 1974; Burke et al., 1982).

TABLE 3. Nd ISOTOPIC COMPOSITION OF MODERN OCEAN WATER AND POTENTIAL Nd SOURCES

Ocean or Crustal Source	ϵ_{Nd} (0)	$f^{Sm/Nd}$
Pacific Ocean	-5 to 0	~-0.4
Atlantic Ocean	-14 to -9	~-0.4
Indian Ocean	-11 to -7	~-0.4
Mid-ocean Ridge Basalts	+8 to +14	~+0.25
Oceanic Islands/Island arcs	+4 to +10	~-0.1 to +0.1
Continental Flood Basalts	-4 to +8	~ 0.1 to +0.1
Old Continental Crust	<-3	~-0.4

Note: ε and f defined in text.

Variations Among Depositional Settings

Figure 3 focuses on the REE patterns of samples from the middle Paleozoic. Sorting out the patterns spatially by general depositional setting and temporally by series within each system reveals a strong similarity between contemporaneous samples from the same environment. Samples from Devonian Pacific coastal regimes show negative Ce anomalies in the Gedinnian and Frasnian, whereas in Famennian time, the Ce depletion temporarily disappears. The negative Ce anomaly returns in Mississippian samples from the Pacific coast. For all Pacific samples, slopes of the heavy lanthanide portion of the patterns are intermediate and consistent within each time frame.

There are only two samples from coastal settings of the Proto-Atlantic: from New York in the Lower Upper Devonian and England in the lowermost Mississippian. The contrasts be-

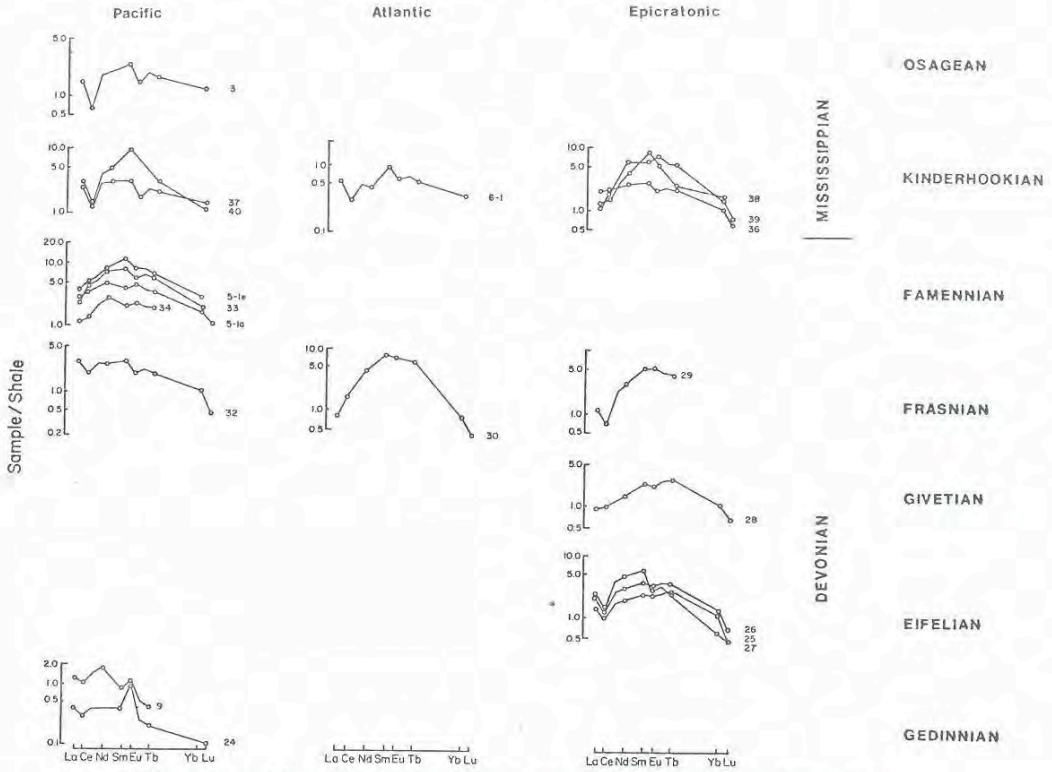

Figure 3. Spatial and temporal distribution of shale-normalized REE in conodonts.

tween them are striking: the Devonian sample has no Ce anomaly and the Mississippian sample does. Heavy lanthanides in the Devonian sample are very depleted, whereas heavy REE in the Mississippian sample are much less depleted.

Comparison of contemporaneous Pacific and Proto-Atlantic samples reveals major differences in Frasnian REE patterns and similarities in Kinderhookian patterns.

Conodont samples from epicratonic seas also show variations in REE distributions through time and in contrast to the other depositional settings, but are consistent among contemporaneous samples.

Interpretation

Any interpretation of variations in REE patterns of fossil biogenic apatite of conodonts and fish, and their relationship to ancient seas and depositional environments, depends on a clear understanding of the interactions of these factors in the modern ocean. Biogenic apatite, during its precipitation within the living organism, can be viewed as a minor flux or site of removal of major and trace element species from the oceanic reservoir. However, fossil biogenic apatite has undergone chemical reactions during decomposition of the surrounding organic matter of the animal, as well as the processes of sedimentation and early diagenesis. Then deep burial, later diagenesis, and lithification have occurred, followed by uplift, possible fracturing of the enclosing rocks, circulation of groundwaters, and erosion. This complex history would seem to imply so many interactions that original seawater relationships would be lost.

Several lines of evidence suggest that the most important reactions occur during primary sedimentation and early diagenesis of biogenic apatite, essentially locking in the trace element characteristics of oceanic bottom waters.

Recent successes in radiometric age dating of conodonts by two separate methods, fission tracks (Sachs et al., 1980) and U-Pb (Kovach and Zartman, 1981), support the hypothesis that early diagenetic processes closely related to seawater composition are the last major influence on TE contents of conodonts. Furthermore, 1) $^{87}Sr/^{86}Sr$ in conodonts (Kovach, 1981) fits the worldwide age curve already determined for calcite of fossil shells (Peterman et al., 1970) and for whole rock limestone (Burke et al., 1982; Veizer and Compston, 1974), and 2) Sr contents from a widespread geographic distribution show a consistent secular decrease during the Paleozoic (Kovach, 1980).

Figure 4 illustrates the relationship between REE in Pacific (Goldberg et al., 1963) and Atlantic (Elderfield and Greaves, 1982) seawater, and biogenic apatite from living fish (this study), and fish debris in sedimentary horizons from 4 to 600 cm on the Pacific abyssal plain (Bernat, 1975). The few analyses available for REE in biogenic apatite in modern living fish (Table 1, sample JWC 20-6, Fig. 4; Table 2, sample Ph-02) indicate that the REE are not significantly enriched during the primary biologic

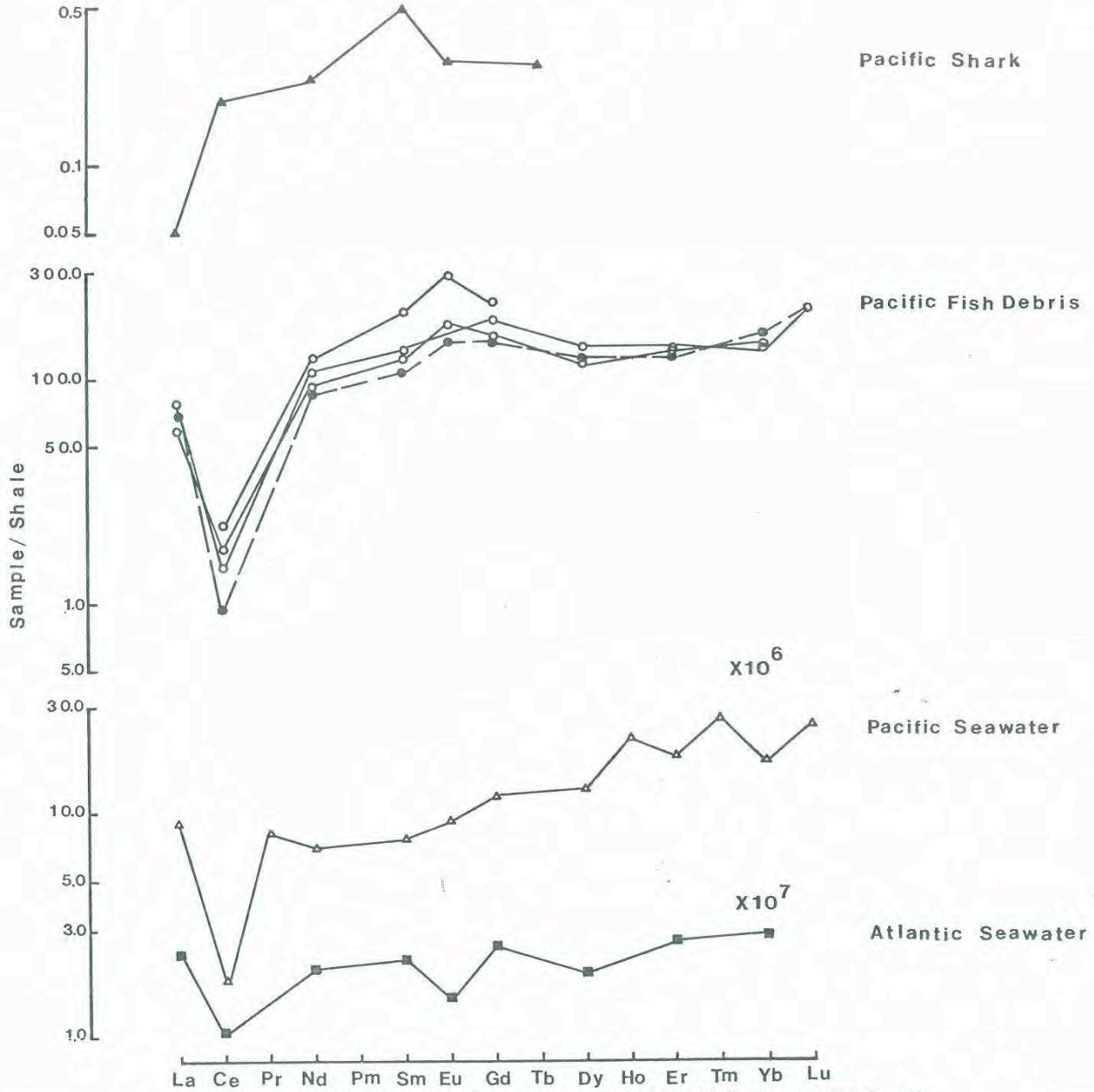

Figure 4. Shale-normalized REE in shark teeth (this study) and fish debris (Bernat, 1974) from the Pacific Ocean, and in seawater from the Pacific (Goldberg et al., 1963) and Atlantic (Elderfield and Greaves, 1982).

production of apatite (see also Shaw and Wasserburg, 1983). Nevertheless, modern biogenic apatite on the sea floor appears to concentrate the REE during early diagenesis by several orders of magnitude over the concentrations actually present in living fish or in oceanic bottom water (Figure 4). Furthermore, trace-element adsorption by biogenic apatite during early diagenesis reproduces the negative cerium anomaly of seawater in the apatite. More importantly, there is almost no fractionation during the adsorption process; i.e., the REE patterns of Pacific fish debris and Pacific bottom water are nearly identical (Figure 4). This suggests that biogenic apatite acquires a signature of the REE content of overlying water masses at the sediment-water interface, although the detailed processes involved are not clear.

Assuming that this implication is valid, and that the negative cerium anomaly and enrichment of heavy lanthanides in modern fish debris are a real record of modern seawater, what factors can

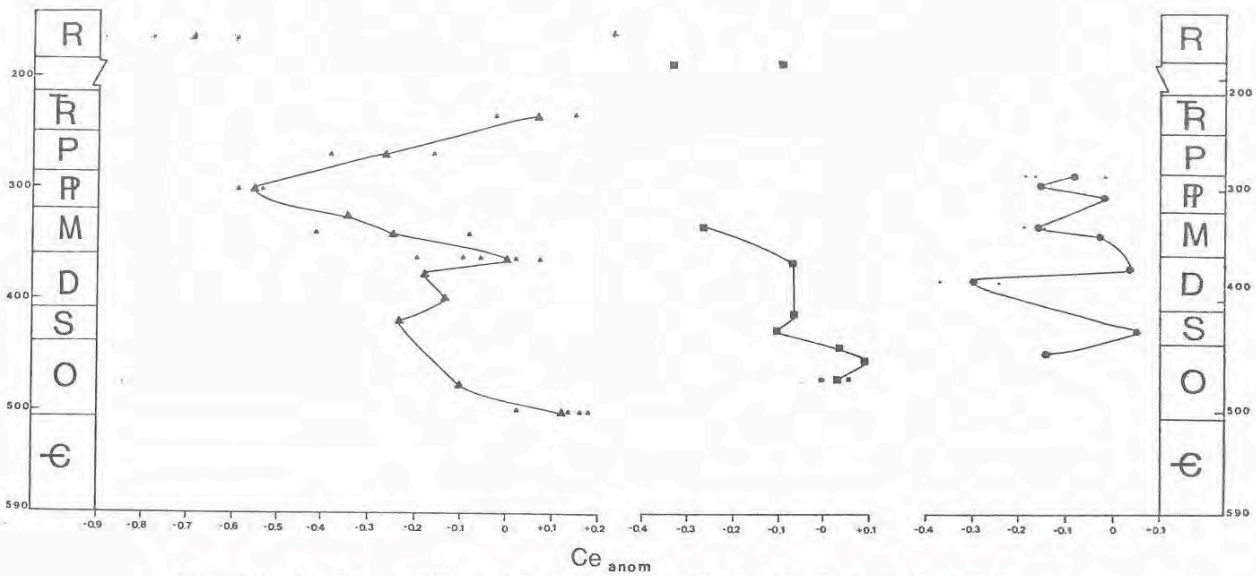

Figure 5. Secular variation of Ce_{anom} (see text for definition) in conodonts by depositional environment, compared to Ce_{anom} of modern Pacific (Goldberg et al., 1963) and Atlantic (Elderfield and Greaves, 1982) seawater, and shark teeth (this study) and fish debris (Bernat, 1974) from the Pacific. Curve is drawn through sample mean; supplementary points show range of values. Triangular shape = Pacific coastal regime, square = Atlantic coastal regime, circle = epicratonic sea (Time scale after Harland et al., 1982). R = Recent.

explain the absence of a cerium anomaly in many conodont samples; e.g., from early Paleozoic time? REE removal from modern seawater appears to be dominated by co-precipitation with colloidal material, mainly iron oxyhydroxide flocs (Turckian et al., 1973; Elderfield and Greaves, 1982; Li, 1981). The process of REE removal is particularly characterized by the affinity of cerium for hydrous iron oxides, so that Ce is preferentially removed by up to a factor of 10 in comparison to the other REE (Elderfield et al., 1981; Mellin, 1981). In the modern ocean oxidizing conditions prevail throughout most of the water column, and Ce is stored preferentially in hydrous iron oxides such as ferromanganese nodules. Demaison and Moore (1980) and Keith (1982) model oceanic environments in which anoxic conditions are widespread. Under such conditions, the oceans are characterized by sulfur-reducing bacteria and H_2S within the water column, as well as by deposition of pyrite in the sediments. In this regime iron oxyhydroxide flocs, if formed in oxidizing surface waters, would dissolve in deeper anoxic water masses, releasing the REE to circulate through the upper sedimentary layers and to become incorporated into biogenic apatite (Wright-Clark and Holser, 1981). This suggests that absence of a Ce anomaly in conodonts records episodes of anoxic conditions in ancient seas.

This hypothesis is supported by correlation of documented Paleozoic anoxic events with the REE patterns from conodonts that do not show a negative Ce anomaly. Erdtmann (1982) relates the deposition of Lower Ordovician Dictyonema-bearing black shales to two types of anoxic environments;. upwelling-anoxic zones and open ocean anoxic layers (Demaison and Moore, 1980). Lower Ordovician conodont REE patterns (Figure 2) contain normal Ce concentrations (do not have a negative Ce anomaly), suggesting that the bottom water anoxia was of sufficient lateral distribution to leave a signature in near-shore carbonate deposits. Berry and Wilde (1978; Wilde and Berry, 1982, ms.) model extensive Cambrian, Ordovician and Silurian black shale sequences that were deposited below mid-water anoxic layers. Oxygenated conditions or "ventilation" gradually increased, producing both episodic anoxia and episodic black shale deposition in the Devonian. The presence of anoxia is reflected in normal, non-depleted Ce (Figure 2) in conodonts of lower Paleozoic shelf carbonate sequences. Variations in Ce in samples from epicratonic seas may reflect changes in water circulation patterns and freshwater/marine input to periodically anoxic silled basins.

Cerium Anomaly

Changes in cerium in relationship to adjacent elements, lanthanum and neodymium, may be defined by:

$$Ce_{anom} = \log (3Ce_n/2La_n + Nd_n)$$

where:

n = shale-normalized value of the REE in a given sample

Ce_{anom} = a quantitative determination of the relative variation of Ce; i.e., enrichment or depletion (after Elderfield and Greaves, 1982).

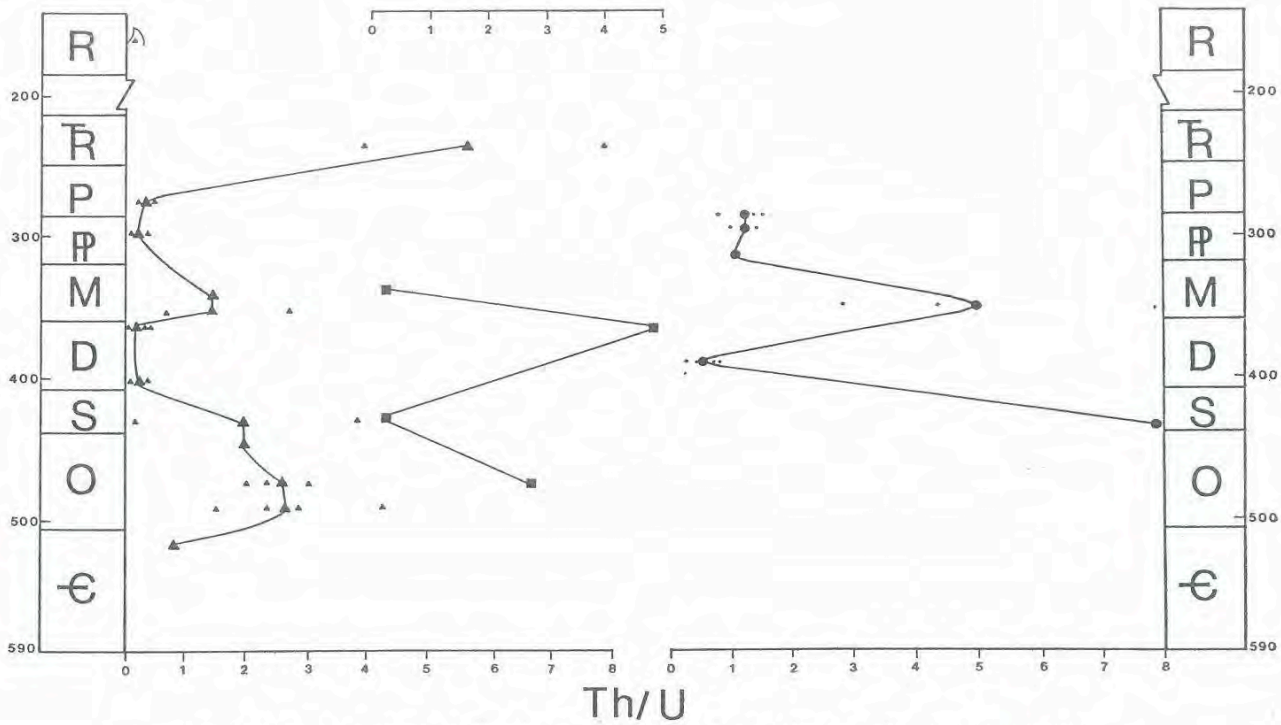

Figure 6. Secular variations in Th/U ratios in conodonts by depositional environment compared to average value of modern seawater (Burton, 1974). Symbols and curve drawn as in Figure 5. Upper scale for Atlantic values. R = Recent.

This definition permits graphical representation of variations of Ce_{anom} values versus stratigraphic horizon or depositional environment, as well as a straightforward comparison among the samples of that aspect of the REE pattern. Ce_{anom} values in Cambrian through Triassic conodonts (Figure 5) reaffirm the variations discussed previously (Figures 2 and 3). Ce_{anom} as a redox indicator yields high values (absence of negative cerium anomaly) during times of anoxic conditions, and low values (presence of negative cerium anomaly) for oxidizing conditions in the water mass that influenced the upper sedimentary layers at the time of deposition. This suggests that anoxic conditions were prevalent in lowermost Paleozoic seas on Atlantic and Pacific margins, began to decline in the Late Ordovician to Silurian, reached another high in the Devonian, and dropped off sharply in the Carboniferous so that aerobic conditions were dominant. Anaerobic water masses began to build up in the Latest Permian to another high in the Triassic. The signal for epicratonic seas shows wide fluctuations, and may reflect a combination of values from many individual basins that were not always interconnected. A more accurate picture will derive from stratigraphically continuous sampling within each basin.

It is interesting to note that Ce_{anom} from Atlantic and Pacific samples correlates positively with $\delta^{34}S$, and negatively with $\delta^{13}C$ (Hoefs, 1981; Saltzmann et al., 1982). This lends support to the hypothesis that many factors (e.g., tectonic activity, transgression-regression, the development of anoxic water masses) interact in positive or negative feedback systems to produce essential changes in the hydrosphere and leave the record of their influence in the sediments and biotic remains deposited at the time (Demaison and Moore, 1980; Keith, 1982).

Thorium to Uranium Ratios

The relative concentrations of thorium and uranium in a sedimentary phase vary according to changes in oxidation-reduction of circulating groundwaters so that complexing agents (PO_4, CO_3, O_2) in aerobic waters mobilize $U^{4+} \rightarrow U^{6+}$, and anaerobic waters reduce and precipitate $U^{6+} \rightarrow U^{4+}$ in insoluble uranium compounds (see Levinson, 1980, for a complete discussion). Because thorium is not mobile in aqueous solution, a systematic variation of Th/U ratios in continental and marine sediments and in seawater has been observed (Adams and Weaver, 1958). Ideally, the balance of these elements in seawater and the availability of uranium during early diagenesis should be controlled by the presence of anoxia within the water column. Thus Th/U should increase during times of anoxia and decrease under anoxic conditions. Empirically this is reflected to a certain extent in conodont samples (Figure 6) as a positive correlation through time between Th/U and Ce_{anom}.

Nd, Sr Isotopic Results

The results of our isotopic analyses of a small number of conodont samples are presented in Table 2. The samples cover the limited time-span of 342-357 My (M. Kinderhookian to L. Frasnian). All of these samples have $\epsilon_{Sr}(T)$ in good agreement with published seawater Sr isotopic curves (Burke et al., 1982) and lie in a restricted range of +53 to +57. The samples also have a very restricted range of $\epsilon_{Nd}(T)$ values from −7.1 to −6.0, suggesting that they share a common source of Nd: seawater. Pacific (JWC-35, −37, and −32) and Proto-Atlantic (JWC-30) samples have approximately the same initial Nd isotopic composition. This may indicate that the Pacific and Proto-Atlantic oceans were well-mixed with respect to the REE at that time, or it may be a coincidence. The moderately negative $\epsilon_{Nd}(T)$ value of ~ -6.5 obtained for these samples requires that this Nd be dominantly from an old source with a time-integrated history of LREE (light REE) enrichment relative to chondrites ($f^{Sm/Nd} < 0$). Specifically, if the source was continental crust with $f^{Sm/Nd} \sim -0.4$, then that crust would be, on average, ~1 AE old today. If the value of ϵ_{Nd} (T) = −6.5 represents a mixture of Nd from continental and oceanic mantle sources, then this 1 AE age represents the minimum age of the continental component. Knowledge of the ϵ_{Nd} (T) variations in ancient seawater would, by similar arguments, place important constraints on the age of the exposed continents as a function of time. It is interesting to note that sample JWC-30 with ϵ_{Nd} (T) = −6.9 has a slightly positive value of $f^{Sm/Nd} = +0.06$. As stated above, a negative value of ϵ_{Nd} (T) requires a time-integrated value of $f^{Sm/Nd} < 0$. It does not appear possible to generate the observed ϵ_{Nd} (T) and $f^{Sm/Nd}$ in this sample by simple mixing of reasonable endmember sources such as those listed in Table 3. Therefore, the REE in this sample were fractionated at some time. This fractionation may have occurred at one or more points in a long chain of events: during a mantle or crustal event such as metamorphism prior to entry of the REE into the weathering cycle, during weathering of the crustal sources, during transport of the REE to the ocean, within the water column, during incorporation of the REE into the conodont, or during the burial history of the conodont. This sample points out the complexities which must be unravelled before a complete understanding of the REE in the weathering and sedimentary cycle can be reached. Nevertheless, this and other preliminary work (Shaw and Wasserburg, 1983; Shaw, 1984) indicate that conodonts together with other sedimentary authigenic and biogenic apatite may be useful in establishing the Nd isotopic variations of ancient seawater.

CONCLUSIONS

Trace element investigations of biogenic apatite of conodonts suggest that a synthesis of the disciplines of geochemistry and biostratigraphy may provide a useful, quantitative approach to determining the variables that affected biota in ancient depositional settings. The principal concepts resulting from our interpretations are:

1) REE patterns of conodonts provide a fingerprint that is specific to contemporaneous samples from the same depositional setting.

2) Fossil apatite may carry a signature of variations in redox conditions, thus recording anoxic events in ancient seas.

3) Ce_{anom} and Th/U curves show secular variations approximately correlative with the age curves of stable isotopes as well as with well-documented anoxic events.

4) Several major extinction events, i.e., Cambrian-Ordovician, Devonian-Mississippian, and Permian-Triassic (Fåhraeus, 1976), occur contemporaneously with anoxic signals retained in conodonts. This suggests that detailed studies of these times will furnish additional clues to the forcing mechanisms involved in evolution.

5) Fossil apatite records Nd isotopic variations in ancient seawater. Curves of ϵ_{Nd} (T) versus age have potential uses in paleooceanography, plate tectonic reconstructions and models of crustal evolution.

ACKNOWLEDGMENTS

Well-characterized sample material (as picked conodonts or whole rocks) from the donors listed in Tables 1 and 2 was an essential contribution to this research. We give very special thanks, for their patience and insight into seawater dynamics and trace element geochemistry during many long discussions, to W. T. Holser, G. J. Wasserburg, G. G. Goles, D. J. Piepgras, and to J. F. Miller for believing that geochemists and biostratigraphers can function symbiotically. Laboratory facilities and irradiation costs were provided by NASA-Johnson Space Center, Houston, with the kind permission of R. J. Williams and D. P. Blanchard. Financial support of the research was by U.S. National Science Foundation Grants EAR 8115985 (to W. T. Holser), and by OCE 8108595 and NASA-NGL05-002-188 (to G. J. Wasserburg). This is Contribution No. 3901(442) of the Division of Geological and Planetary Sciences, California Institute of Technology, Pasadena, California.

APPENDIX 1. Th, U, AND REE IN CONODONTS AND SHARK TEETH (ppm)*

Age	Sample	Expt.	Th	U	La	Ce	Nd	Sm	Eu	Tb	Yb	Lu
Modern												
	JWC20-6	NASA	n.d.	n.d.	1.99	14.7	9.	6.	0.58	0.36	0.28	0.034
					0.07	0.3	3.	2.	0.02	0.03	0.11	0.019
Triassic												
	JW6	UofO	4.3	n.d.	24.2	58.	n.d.	6.14	0.90	0.85	n.d.	n.d.
		59	0.3		0.5	5.		0.07	0.09	0.06		
	JWC56	NASA	32.1	n.d.	107.	369.	178.	33.1	5.9	4.40	3.9	0.35
		184	1.3		2.	7.	11.	0.6	0.3	0.15	0.3	0.05
	JWC9-1	NASA	2.5	n.d.	18.9	55.	n.d.	n.d.	1.9	n.d.	n.d.	n.d.
		193	1.0		0.7	9.			0.2			
Permian												
	JW5a	UofO	n.d.	n.d.	35.	n.d.	n.d.	8.9	n.d.	n.d.	n.d.	n.d.
		59			3.			0.3				
	JW5b	UofO	27.3	59.	201.	159.	n.d.	46.8	8.2	4.5	n.d.	n.d.
		59	1.8	8.	4.	10.		0.6	1.1	0.7		
	JWC54	NASA	20.7	55.	202.	158.	181.	54.8	8.6	7.8	8.8	0.95
		184	0.9	4.	5.	14.	14.	1.	0.8	0.8	0.8	0.09
Pennsylvanian												
	JWC51	NASA	4.71	13.8	43.8	89.8	50.	15.4	3.63	2.34	2.81	0.41
		184	0.19	0.7	0.9	1.6	3.	0.3	0.09	0.07	0.14	0.03
	JWC50	NASA	n.d.	n.d.	28.	47.3	45.	2.48	2.6	1.32	n.d.	n.d.
		192			2.	1.8	13.	0.11	0.08	0.14		
	JWC47	NASA	7.2	7.	n.d.	48.	49.	10.8	1.91	2.3	2.8	n.d.
		192	0.9	2.		2.	22.	1.6	0.10	0.2	0.5	
	JWC46	"	9.9	n.d.	48.	83.	90.	19.	3.89	n.d.	4.4	0.43
			1.7		3.	3.	30.	2.	0.15		0.5	0.19
	JWC45	NASA	4.9	6.0	16.8	38.5	n.d.	7.68	2.00	1.03	1.57	0.22
		184	0.2	0.5	0.4	1.5		0.13	0.05	0.14	0.17	0.04
	JWC41	NASA	4.8	5.6	27.5	54.	60.	9.5	3.20	1.68	2.0	n.d.
		192	1.1	1.2	1.8	2.	20.	0.2	0.13	0.19	0.3	
	JWC52	NASA	0.91	6.2	64.8	29.5	24.	9.70	5.09	1.10	2.1	0.18
		184	0.09	0.6	1.3	0.9	3.	0.17	0.14	0.13	0.2	0.02
	JWC53	NASA	n.d.	40.	970.	436.	600.	117.4	29.4	12.3	47.	37.
		192		16.	20.	19.	200.	1.1	1.4	1.6	5.	1.
	JW4a	UofO	n.d.	8.7	103.	52.	n.d.	14.38	6.5	2.2	3.9	0.56
		59		1.3	3.	4.		0.19	0.8	0.2	0.4	0.06
	JW4b	"	10.1	n.d.	970.	444.	n.d.	122.3	27.	14.5	39.	6.6
			0.7		20.	11.		1.4	2.	0.4	2.	0.3
	JW4c	"	1.40	8.2	90.2	n.d.	n.d.	13.7	n.d.	n.d.	3.2	0.54
			0.15	1.1	1.7			0.2			0.2	0.03
	JWC43	NASA	2.02	3.8	22.9	50.8	33.	10.01	1.01	0.83	1.56	0.17
		184	0.12	0.4	0.4	1.9	6.	0.17	0.06	0.06	0.06	0.03
Mississippian												
	JWC40	NASA	7.3	5.	118.	100.	108.	21.4	3.24	2.6	4.4	0.40
		192	1.6	2.	2.	3.	17.	0.2	0.12	0.3	0.5	0.15
	JW3	UofO	33.3	52.	65.	47.	n.d.	22.4	4.3	n.d.	n.d.	1.29
		59	1.2	7.	2.	5.		0.3	0.8			0.13
	JWC6-1	NASA	0.45	3.8	21.9	21.6	16.	11.45	1.17	0.67	1.0	n.d.
		193	0.08	1.2	0.3	0.5	4.	0.10	0.03	0.06	0.15	

APPENDIX 1. Th, U, AND REE IN CONODONTS AND SHARK TEETH (continued)
(ppm)*

Age	Sample	Expt.	Th	U	La	Ce	Nd	Sm	Eu	Tb	Yb	Lu
Mississippian												
	JWC39	NASA	51.	12.4	41.3	131.	211.	41.1	14.6	7.2	5.03	0.43
		184	2.	0.6	0.8	3.	6.	0.7	0.5	0.3	0.13	0.02
	JWC38	NASA	63.	28.	44.4	110.	143.	88.	10.8	3.0	5.6	n.d.
		192	5.	10.	1.4	4.	30.	8.	.3	.4	0.6	
	JWC37	"	n.d.	n.d.	104.	93.	160.	9.	n.d.	3.7	3.6	n.d.
					6.	6.	30.	0.2		0.4	0.4	
	JWC36	NASA	7.8	0.91	77.9	159.	97.	19.5	4.16	2.78	3.63	0.35
		184	0.3	0.19	1.6	3.	6.	0.4	0.15	0.10	0.16	0.02
	JWC35	"	35.3	15.2	124.	228.	168.	38.5	6.2	4.1	3.8	0.63
			1.4	1.7	2.	5.	17.	1.1	0.4	0.5	0.2	0.06
Devonian												
	JWC5-1a	NASA	2.9	17.	84.1	205.	90.	24.7	7.5	5.1	4.1	0.46
		193	0.7	4.	0.9	4.	30.	0.3	0.3	0.4	0.3	0.11
	JWC5-1b	"	3.1	20.	114.	180.	210.	54.1	11.0	7.5	6.1	0.58
			0.6	4.	3.	20.	100.	0.4	0.2	0.5	0.4	0.10
	JWC5-1e	NASA	10.	39.	174.	446.	402.	110.4	18.3	9.4	8.2	0.65
		192	3.	14.	3.	6.	40.	0.6	0.5	0.8	1.0	0.18
	JWC5-1f	"	13.	36.	143.	390.	300.	80.3	16.	8.7	9.4	n.d.
			5.	13.	3.	10.	30.	0.4	0.5	0.9	1.4	
	JWC34	NASA	n.d.	n.d.	44.	102.	100.	14.3	4.41	2.4	n.d.	n.d.
		192			3.	4.	30.	0.2	0.19	0.3		
	JWC33	"	5.8	n.d.	104.	261.	170.	27.	8.8	4.5	5.6	n.d.
			1.7		8.	6.	40.	7.	0.4	0.5	0.8	
	JWC32	"	n.d.	12.	118.	142.	97.	20.	3.67	2.4	3.6	0.27
				4.	2.	2.	16.	2.	0.11	0.2	0.3	0.11
	JWC30	NASA	4.79	1.01	31.1	124.	153.	54.3	13.9	7.7	2.58	0.238
		184	0.19	0.6	0.6	3.	5.	0.9	0.5	0.2	0.11	0.014
	JWC29	NASA	n.d.	n.d.	45.	52.	n.d.	36.5	10.6	5.2	n.d.	n.d.
		192			3.	3.		0.3	0.3	0.4		
	JWC28	NASA	2.46	3.3	35.3	72.3	53.	15.6	4.09	3.40	3.53	0.36
		184	0.12	0.4	0.7	1.6	4.	0.3	0.12	0.11	0.18	0.03
	JWC27	"	3.52	5.1	55.9	70.9	73.	16.6	4.58	3.30	2.07	0.266
			0.14	0.5	1.1	1.4	3.	0.6	0.13	0.10	0.16	0.016
	JWC26	"	3.9	5.7	85.4	92.	103.	25.8	6.44	4.6	4.5	0.41
			0.2	0.6	1.9	2.	6.	0.4	0.19	0.5	0.2	0.04
	JWC25	NASA	11.5	47.	95.	103.	170.	39.	5.53	3.3	4.0	0.25
		192	1.3	16.	2.	2.	20.	6.	0.17	0.3	0.5	0.10
	JWC24	NASA	0.82	7.46	15.1	21.8	n.d.	3.26	1.78	0.26	n.d.	0.06
		184	0.11	0.07	0.4	1.3		0.08	0.07	0.03		0.03
	JW9	UofO	1.64	4.5	44.9	72.	62.	5.43	2.04	0.50	n.d.	n.d.
		57	0.2	0.3	0.8	3.	2.	0.07	0.19	0.06		
Silurian												
	JWC23	NASA	21.	n.d.	139.	331.	300.	78.3	15.4	8.0	6.6	0.42
		192	3.		3.	5.	30.	0.5	0.8	0.7	0.7	0.19
	JWC4-1	NASA	10.9	n.d.	160.	513.	360.	122.	22.1	15.4	11.8	0.98
		193	1.3		3.	9.	90.	17.	1.9	1.1	0.8	0.16
	JW8	UofO	47.6	12.8	179.	373.	604.	60.	6.2	5.8	2.6	0.38
		57	1.7	0.9	3.	11.	18.	0.7	0.4	0.2	0.4	0.03

APPENDIX 1. Th, U, AND REE IN CONODONTS AND SHARK TEETH (continued)
(ppm)*

Age	Sample	Expt.	Th	U	La	Ce	Nd	Sm	Eu	Tb	Yb	Lu
Silurian												
	JW10	UofO	5.1	29.9	25.4	79.	n.d.	20.6	3.2	n.d.	n.d.	1.02
		63	0.3	1.6	0.5	3.		0.2	0.3			0.05
	JW11	"	4.2	11.1	69.2	210.	n.d.	24.7	6.89	n.d.	n.d.	0.37
			0.4	0.8	1.2	18.		0.3	0.8			0.05
	JWC22	NASA	87.	n.d.	137.	370.	430.	100.	24.	9.0	12.8	0.9
		192	4.		3.	8.	80.	2.	0.8	0.9	1.3	0.4
	JWC21	NASA	97.	12.2	179.	594.	423.	93.1	21.3	16.2	9.7	0.84
		184	4.	1.2	3.	11.	16.	1.7	0.7	1.7	0.5	0.07
Ordovician												
	JWC20	"	2.16	n.d.	57.4	118.	52.	9.67	2.76	2.01	1.8	0.17
			0.15		1.2	11.	5.	0.16	0.11	0.19	0.2	0.02
	JWC19	NASA	2.7	n.d.	56.5	102.	n.d.	11.3	2.2	1.8	1.9	n.d.
		192	1.1		1.2	5.		0.2	0.3	0.3	0.5	
	JWC18	"	n.d.	n.d.	31.	82.	n.d.	2.94	1.88	1.13	n.d.	n.d.
					2.	3.		0.13	1.2	0.19		
	JWC17	NASA	4.60	2.2	54.2	61.6	22.	6.95	1.33	0.85	2.53	0.20
		184	0.18	0.6	1.2	1.8	4.	0.13	0.06	0.04	0.03	0.02
	JW2a	UofO	18.	n.d.	95.	194.	n.d.	14.52	n.d.	n.d.	n.d.	n.d.
		59	2.		2.	17.		0.19				
	JW2b	"	40.1	n.d.	98.	206.	n.d.	20.6	3.5	n.d.	n.d.	n.d.
			1.4		2.8	8.		0.3	0.4			
	JWC16	NASA	36.	13.	90.	352.	250.	82.	12.4	6.5	7.4	0.57
		192	4.	5.	2.	5.	20.	8.	0.4	0.5	0.8	0.17
	JWC3-16	NASA	17.4	n.d.	66.	182.	110.	63.	8.1	5.4	3.4	0.25
		193	0.7		1.	4.	30.	11.	0.7	0.4	0.3	0.09
	JWC15	NASA	14.1	n.d.	25.	78.	100.	5.7	5.2	2.3	4.0	n.d.
		192	1.1		3.	5.	40.	0.2	0.2	0.3	1.8	
	JWC14	NASA	4.66	1.98	76.8	387.	421.	91.0	16.6	8.6	2.10	0.24
		184	0.19	0.13	1.3	7.	13.	1.5	0.5	0.3	0.04	0.02
	JWC3-34	NASA	9.9	n.d.	102.6	274.	180.	47.	6.7	2.8	3.2	n.d.
	Br	193	0.9		1.5	6.	50.	17.	0.8	0.3	0.5	
	JWC3-24	"	34.9	13.	156.1	479.	180.	120.	9.5	6.3	5.9	0.51
	Br		1.0	3.	1.6	5.	40.	20.	0.8	0.4	0.4	0.08
Cambrian												
	JW7	UofO	9.3	10.7	501.	1200.	n.d.	197.	17.5	24.	11.4	1.38
		59	0.7	1.6	10.	20.		2.	1.6	0.6	0.9	0.10

Note: *error = 1σ, n.d. = not detected.

REFERENCES CITED

Adams, J.A.S., and Weaver, C. E., 1958, Thorium-to-uranium ratios as indicators of sedimentary processes: example of concept of geologic facies: Bulletin of the American Association of Petroleum Geologists, 42:387–430.

Bernat, M., 1975, Les isotopes de l'uranium et du thorium et les terres rares dans l'environment marin: Cahiers ORSTOM Séries Geology, 7:65–83.

Berry, W.B.N., and Wilde, P., 1978, Progressive ventilation of the oceans—an explanation for the distribution of the Lower Paleozoic black shales: American Journal of Science, 278:257–275.

——1983, Evolutionary and geologic consequences of organic carbon fixing in the primitive anoxic ocean: Geology, 11:141–145.

Bradshaw, L. E., Noel, J. A., and Larson, R. J., 1973, Neutron activation analysis of selected conodonts, p. 67–84, *in* Rhodes, F.H.T., ed., Conodont Paleozoology: Geological Society of America Special Paper 141, Boulder, Colo.

Brunfelt, A. O., and Steinnes, E., eds., 1971, Activation Analysis in Geochemistry and Cosmochemistry: Proc. of the NATO Advanced Study Institute, Kjeller, Norway, Sept. 1970, Universitetsforlaget, Oslo.

Burke, W. H., Denison, R. E., Heatherington, E. A., Koepnick, R. B., Nelson, H. F., and Otto, J. B., 1982, Variation of seawater $^{87}Sr/^{86}Sr$ throughout Phanerozoic time: Geology, 10:516–519.

Burton, J. D., 1975, Radioactive nuclides in the marine environment, p. 91–192, *in* Riley, J. P., and Skirrow, G., eds., Chemical Oceanography, Vol. 3, p. 91–192: Academic Press, London.

Dasch, E. J., and Biscaye, P. E., 1971, Isotopic composition of strontium in Cretaceous-to-Recent pelagic foraminifera: Earth and Planetary Science Letters, 11:201–204.

Demaison, G. J., and Moore, G. T., 1980, Anoxic environments and oil source bed genesis: Bulletin of the American Association of Petroleum Geologists, 64:1179–1209.

DePaolo, D. J., 1978, Study of magma sources, mantle structure and the differentiation of the earth using variations of $^{143}Nd/^{144}Nd$ in igneous rocks [Ph.D. Dissertation]: California Institute of Technology, Pasadena, California, 360 p.

——and Wasserburg, G. J., 1976, Inferences about magma sources and mantle structure from variations of $^{143}Nd/^{144}Nd$: Geophysical Research Letters, 3:743–746.

Elderfield, H., Hawkesworth, C. J., Greaves, M. J., and Calvert, S. E., 1981, Rare earth element geochemistry of oceanic ferromanganese nodules and associated sediments: Geochimica et Cosmochimica Acta, 45:513–528.

——and M. J. Greaves, 1982. The rare earth elements in seawater. Nature, 296:214–219.

Erdtmann, B-D., 1982, Paleobiogeography and environments of planktic dictyonemid graptolites during the earliest Ordovician, p. 9–27, *in* Bassett and Dean, W. T., eds., The Cambrian-Ordovician Boundary: Sections, Fossil Distributions, and Correlations: National Museum of Wales, Geology Series Number 3, Cardiff.

Fåhraeus, L. E., 1976, Conodontophorid ecology and evolution related to global tectonics, p. 11–26, *in* Barnes, C. R., ed., Conodont Paleoecology: Geological Association of Canada Special Paper 15, Waterloo, Ontario.

Goldberg, E. D., Koide, M., Schmitt, R. A., and Smith, R. H., 1963, Rare-earth distributions in the marine environment: Journal Geophysical Research, 68:4209–4217.

Goldstein, S. L., and O'Nions, R. K., 1981, Nd and Sr isotopic relationships in pelagic clays and ferromanganese deposits: Nature, 292:324–327.

Gordon, G. E., Rundle, K., Goles, G. G., Corliss, J. B., Benson, M. H., and Oxley, S. S., 1968, Instrumental activation analysis of standard rocks with high-resolution γ ray detectors: Geochimica et Cosmochimica Acta, 32:369–396.

Harland, W. B., Cox, A. V., Llewellyn, P. G., Pickton, C.A.G., Smith, A. G., and Walters, R., 1982, A Geologic Time Scale: Cambridge University Press, New York, 128 p.

Haskin, L. A., Haskins, M. A., Frey, F. A., and Wildeman, T. R., 1968, Relative and absolute terrestrial abundance of the rare earths, p. 889–912, *in* Ahrens, L. H., ed., Origin and Distribution of the Elements, Vol. 30: Pergamon Press, London.

——and Paster, T. P., 1979, Geochemistry and mineralogy of the rare earths, p. 1–80, *in* Gschneidner, K. A., Jr., and Eyring, L., eds., Handbook on the Physics and Chemistry of the Rare Earths, Vol. 3: North-Holland Publishing Company, New York.

Hoefs, J., 1981, Isotopic composition of the ocean-atmosphere system in the geologic past: American Geophysical Union Geodynamics Series 5:110–118.

Jacobsen, S. B., and Wasserburg, G. J., 1980, Sm-Nd isotopic evolution of chondrites: Earth and Planetary Science Letters, 50:139–155.

Keith, M. L., 1982, Violent volcanism, stagnant oceans and some inferences regarding petroleum, strata-bound ores and mass extinctions: Geochimica et Cosmochimica Acta, 46:2621–2637.

Kovach, J., 1980, Variations in the strontium isotopic composition of seawater during Paleozoic time determined by the analysis of conodonts: Geological Society of America Abstracts with Programs, 12:465.

——1981, The strontium content of conodonts and possible use of the strontium concentrations and strontium isotopic composition of conodonts for correlation purposes: Geological Society of America Abstracts with Programs, 13:285.

——and Zartman, R. W., 1981, U-Th-Pb dating of conodonts: Geological Society of America Abstracts with Programs, 13:285.

Levinson, A. A., 1980, Introduction to Exploration Geochemistry, the 1980 Supplement: Applied Publishers, Wilmette, Ill., 924 p.

Li, Y-H, 1981, Ultimate removal mechanisms of elements from the ocean: Geochimica et Cosmochimica Acta, 45:1659–1664.

Lowenstam, H. A., 1974, Impact of life on chemical and physical processes, p. 715–796, *in* Goldberg, E. D., ed., The Sea, Vol. 5, Marine Chemistry: John Wiley and Sons, New York.

——and Weiner, S., 1983, Mineralization by organisms and the evolution of biomineralization, p. 191–203, *in* Westbroek, P., and de Jong, E. W., eds., Biomineralization and Biological Metal Accumulation: D. Reidel Publishing Company, New York.

Mellin, T.A.M., 1981, Structural chemistry of synthetic manganate and iron compounds: implications for geochemistry of marine ferrimanganese deposits [Ph.D. Dissertation]: University of California at San Diego, Department of Marine Geology: University of Goteborg, Sweden, No. 1, 237 p.

Muecke, G., ed., 1980, Short Course in Neutron Activation Analysis in the Geosciences: Mineralogical Association of Canada, Halifax, 279 p.

O'Nions, R. K., Hamilton, P. J., and Evensen, N. M., 1977, Variations in $^{143}Nd/^{144}Nd$ and $^{87}Sr/^{86}Sr$ ratios in oceanic basalts: Earth and Planetary Science Letters, 34:13–22.

Papanastassiou, D. A., Depaolo, D. J., and Wasserburg, G. J., 1977, Rb-Sr and Sm-Nd chronology and genealogy of basalts from the Sea of Tranquility: Proceedings of the Lunar Science Conference, 8:1639–1672.

Peterman, Z. E., Hedge, C. E., and Tourtelot, H. A., 1970, Isotopic composition of strontium in seawater throughout Phanerozoic time: Geochimica et Cosmochimica Acta, 34:105–120.

Piepgras, D. J., and Wasserburg, G. J., 1980, Neodymium in isotopic variations in seawater: Earth and Planetary Science Letters, 50:128–138.

——1982, Isotopic composition of neodymium in waters from the Drake Passage: Science, 217:207–218.

——and Dasch, E. J., 1979, The isotopic composition of Nd in different ocean masses: Earth and Planetary Science Letters, 45:223–236.

Sachs, H. M., Denkinger, M., Bennett, C. L., and Harris, A. G., 1980, Radiometric dating of sediments using fission tracks in conodonts: Nature, 288:359–361.

Saltzman, E. S., Lindh, T. B., and Holser, W. T., 1982, $\delta^{13}C$ and $\delta^{34}S$, global sedimentation, $p0_2$, and $pC0_2$ during the Phanerozoic: Geological Society of America Abstracts with Programs, 14:607.

Shaw, H. F., 1984, Sm-Nd and Rb-Sr isotopic systematics of tektites and other impactites, Appalachian mafic rocks, and marine carbonates and phosphates [Ph.D. Dissertation]: California Institute of Technology, Pasadena, California, 282 p.

——and Wasserburg, G. J., 1983, Sm, Nd in modern and ancient marine $CaCO_3$ and apatite [Abstract]: EOS, Trans., American Geophysical Union, 64:335.

Taylor, S. R., and McLennan, S. M., 1981, The rare earth element evidence in Precambrian sedimentary rocks: implications for crustal evolution, p. 527–548, *in* Kroner, A., ed., Precambrian Plate Tectonics: Elsevier, Amsterdam.

Turekian, K. K., Katz, A., and Chan, L., 1973, Trace element trapping in pteropod tests: Limnol. and Oceanography, 18:240.

Veizer, J., and Compston, W., 1974, $^{87}Sr/^{86}Sr$ composition of seawater during the Phanerozoic: Geochimica et Cosmochimica Acta, 38:1461–1484.

——Holser, W. T., and Wilgus, C. K., 1980, Correlation of $^{13}C/^{12}C$ and $^{34}S/^{32}S$ secular variations: Geochimica et Cosmochimica Acta, 31:2181–2196.

Wasserburg, G. J., Jacobsen, S. B., Depaolo, D. J., McCulloch, M. T., and Wen, T., 1981, Precise determination of Sm/Nd ratios: Sm and Nd isotopic abundances in standard solutions: Geochimica et Cosmochimica Acta, 45:2311–2323.

Wilde, P., and Berry, W.B.N., 1982, Progressive ventilation of the oceans-potential for return to anoxic conditions in the post-Paleozoic, p. 209–224, *in* Schlanger, S. O., and Cita, M. B., eds., Nature and Origin of Cretaceous Carbon Rich Facies: Academic Press, London.

——(in press), Destabilization of the oceanic density structure and its significance to marine extinction events: Submitted to the Bulletin of the Geological Society of America.

Wright-Clark, J., and Holser, W. T., 1981, REE in conodont apatite as a measure of redox conditions in ancient seas: Geological Society of America Abstracts with Programs, 13:586.

MANUSCRIPT ACCEPTED BY THE SOCIETY JUNE 5, 1984

Typeset by WESType Publishing Services, Inc., Boulder, Colorado
Printed in U.S.A. by Malloy Lithographing, Inc., Ann Arbor, Michigan